A theoretical investigation of the effect of fluorination and bromination on the optoelectronic properties of tetrathienophenazine derivatives

Koussai Lazaar, Saber Gueddida, Dietrich Foerster, Moncef Said

A theoretical investigation of the effect of fluorination and bromination on the optoelectronic properties of tetrathienophenazine derivatives

Koussai Lazaar[a,b], Saber Gueddida[c,*], Dietrich Foerster[b], Moncef Said[a]

[a] *Université de Monastir, Faculté des Sciences de Monastir, Laboratoire de la Matière Condensée et des Nanosciences (LMCN), LR11ES40, Avenue de l'Environnement 5000 Monastir, Tunisie.*
[b] *Univ. Bordeaux, LOMA, CNRS UMR7598, F-33400 Talence, France.*
[c] *Univ. Lorraine, LPCT, CNRS UMR7019, F-54506 Vandoeuvre-Les-Nancy, France.*

Abstract

The electronic and optical properties of crystalline tetrathienophenazine derivatives (l-TTP, m-TTP, t-TTP) and their four fluorinated and brominated derivatives are predicted using density functional theory within the generalized gradient approximation and including the van der Waals weak interactions. We analyze how the position of sulfur atoms and fluorination and bromination modify the charge transport in TTP derivatives. Our results show that the introduction of bromine substituents into TTP derivatives has a stronger effect than fluorination. The introduction of the fluorine atoms improves the hole transport in the l-TTP derivatives, while bromine atoms improve both hole and electron transport of the three TTP derivatives. Our findings suggest a new series of promising ambipolar organic materials.

1. Introduction

Organic semiconductors (OSCs) based on π-conjugated materials have attracted considerable attention during the last decade due to their potential applications in organic light-emitting diodes (OLED) [1, 2, 3, 4], organic field-effect transistors (OFET) [5, 6, 7, 8, 9, 10] and organic photovoltaic (OPV)[11, 12, 13, 14, 15, 16] cells. They can be used in large area devices and flexible substrates and the rich choice of conjugated molecules as constituents and their low cost of fabrication make them good alternatives to conventional inorganic materials [17, 18, 19, 20]. So far, however, few n type semiconductors with a sufficient electron mobility were found [21, 22]. Therefore, several experimental and theoretical studies have been developed in order to synthesize high performance n-type organic semiconductors [22, 23, 24]. The functionalization of p-type organic semiconductors with electron-withdrawing groups such as Cl, F and Br atoms was found to be a promising way

*I am corresponding author
Email address: saber.gueddida@univ-lorraine.fr (Saber Gueddida)

to convert them into n-type semiconductors [25, 26]. It has been shown that slight chemical modifications of organic molecules such as changing the location of a heteroatom, introducing different substituents and alternative π-conjugated cores change their optical and electrochemical behavior [27, 22, 28, 19, 29].

The oligothiophenes, the linear arenes and their derivatives are the most widely studied organic semiconductors among all π-conjugated materials due to their large π-conjugation and outstanding chemical and physical properties [22, 27]. In a recent study, a series of TTP derivatives (l-TTP, m-TTP, t-TTP) have been synthesized via a simple condensation reaction between diketones and diamines [30]. The optical and electronic properties of these molecules were investigated using ab initio density functional theory calculations at the B3LYP level by Y. Xie et al [30]. It has been shown that the position of the sulfur atoms changes the frontier molecular orbitals, reorganization energies and their transport properties [30]. The energy levels of the lowest unoccupied molecular orbital (LUMO) were found to be -2.27 eV, -2.33 eV and -2.39 eV for l-TTP, m-TTP and t-TTP isomers, respectively. The ordering of the LUMO energy levels follows the same progression as those of the highest occupied molecular orbital (HOMO), while the difference between the LUMO levels was slightly larger than that of the HOMO ones. Therefore, the HOMO-LUMO gaps in these molecules are in the order l-TTP $>$ m-TTP $>$ t-TTP [30]. Attaching electron-withdrawing substituents such as Br and F atoms to the π conjugated ring modifies the molecular geometry and electronic properties [22, 23, 24]. It was shown that the introduction of fluorine atoms on anthra-tetrathiophen (ATT) molecules does not affect their planarity but reduces the HOMO-LUMO gap, which is beneficial to electron injection and provides more charge carrier stabilization [22, 28, 31, 32]. In another approach, a small change of the intermolecular hole reorganization energy is found when replacing the hydrogen moieties of ATT derivatives with bromine substituents [27].

To our knowledge, the crystal structures of the known TTP derivatives (l-TTP, m-TTP, t-TTP) and their fluorinated and brominated derivatives have not yet been studied by ab initio methods. The aim of the present work is to predict the optical, electronic and transport properties of these crystal structures, and to investigate the effect of changing the position of sulfur atoms and the number and location of electron-withdrawing groups such as fluorine and bromine atoms on their properties. We will propose a series of new high performance n and/or p type organic semiconductors.
Our paper is organized as follows: in the first part we briefly describe our calculation methods, and in the second part we present our results for the l-TTP, m-TTP and t-TTP crystal structures and their fluorinated and brominated derivatives. We first describe the structural properties and then discuss the electronic properties of the molecular and crystal structures of TTP derivatives. Finally, we present their optical properties based on their dielectric functions.

2. Method of calculation

The molecular and periodic calculations conducted in this work were performed using the SIESTA DFT (Density Functional Theory [35]) package [33, 34] that uses atomic orbitals as basis functions and the generalized gradient approximation (GGA). The Perdew-Burke-Ernzerhof (PBE) exchange-correlation density functional was used [36]. Norm-conserving pseudopotentials of Troullier and Martins were used to describe the core electrons [37, 38]. A DZP basis set, and energy cutoffs of 100 Ry for m-TTP and l-TTP derivatives, and 120 Ry for t-TTP derivatives were used. The pseudo atomic orbitals (PAOs) in the SIESTA code [33, 34] are radially confined by using an energy shift in each orbital of 0.001 Ry. van der Waals interactions were included for selected crystal structures by means of the DFT-D2 correction by Grimme and co-workers [39]. The total energy for both molecular and periodic calculations was converged to $5\times\ 10^{-6}$ Hartree. The integration over the Brillouin zone was sampled by $2\times2\times2$ k-points for l-TTP, $2\times4\times1$ k-points for m-TTP and $2\times5\times2$ k-points for t-TTP, using the Monkhorst-Pack scheme [40]. For molecular systems, 3 nm of vacuum was used to separate the periodically repeated molecules in order to avoid interactions between them. Periodic boundary conditions were applied in all space directions for both molecular and crystal structures. The structural relaxations of both molecular and crystal systems were performed by nullifying the force on the atoms with a precision of 10^{-5} Ry/Å. All atoms of different isomers are relaxed, for both molecules and crystals. In the calculation of the dielectric properties, an optical broadening of 0.1 eV was chosen. The imaginary part of the dielectric function is obtained by computing the dipolar transition matrix elements between the occupied and unoccupied states, while the real part is determined using the Kramers-Kroning transformations [41].

3. Results and discussion

3.1. Structural properties

Three molecular isomers of tetrathienophenazine (TTP) [30] are considered in this work: l-TTP, m-TTP and t-TTP. Each one contains 34 atoms; 2 nitrogen, 4 sulfur, 20 carbon and 8 hydrogen atoms. For each molecular model, introducing fluorine and bromine substituents depending on their number and their locations has generated 4 derivatives. Figure 1 shows the molecular structure of the l-TTP, m-TTP and t-TTP isomers and their fluorinated and brominated isomers. The difference in the three isomers l-TTP, m-TTP and t-TTP (with $R_1 = R_2 = R_3 = R_4 = H$) is in the position of the 4 sulfur atoms. The sulfur atoms are positioned outside in l-TTP (Figure 1 left panel) and inside in t-TTP (Figure 1 right panel). However, for the m-TTP molecule, two sulfur atoms are positioned outside and two inside (Figure 1 middle panel). For each TTP derivative, three fluorinated TTP molecules (TTP1, TTP2 and TTP3) and a brominated one (TTP4) are optimized by means of the GGA/PBE functional. For both TTP1 and TTP2, two fluorine atoms were introduced at the positions ($R_2 = R_4 = F$) and ($R_1 = R_3 = F$), respectively. By contrast, the TTP3 and TTP4 isomers were obtained by introducing four atoms of fluorine and bromine at $R_1 = R_2 = R_3 = R_4 = F$ and $R_1 = R_2 = R_3 = R_4 = Br$, respectively.

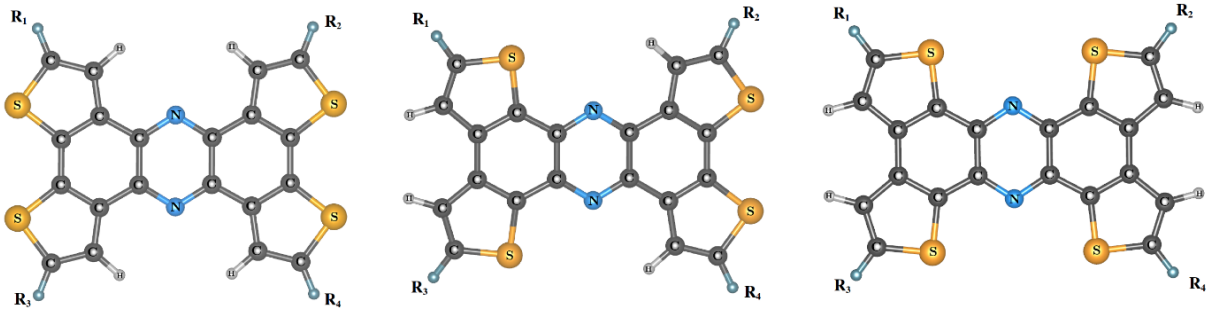

Figure 1: Molecular structure of l-TTP (left panel), m-TTP (middle panel) and t-TTP (right panel) isomers and their electron-withdrawing substituents (F, Br).

After finding the most stable configuration of the isolated molecule for each derivative, we optimized their crystal structure with respect to their total energies. Top and side views of crystals of l-TTP, m-TTP and t-TTP are given in Figure 2. The l-TTP, m-TTP and t-TTP derivatives and their substituded derivatives crystallized in the monoclinic structures $P_{2_1/a}$, P_{2_1} and $P_{2_1/n}$, respectively. The box dimensions of each derivative are summarized in Table 1. The crystal structure of the l-TTP model contains four molecules in their primitive cell, it consists of two columns of slipped $\pi - \pi$ stacked molecules along the b axis with a $\pi - \pi$ intermolecular distance of 3.47Å. The $S - S$ distance in the l-TTP crystal was found to be 3.60 Å. By contrast, the crystal structure of m-TTP and t-TTP isomers contains two molecules, where the $\pi - \pi$ intermolecular distances are found to be 3.49 Å and 3.71Å, respectively.

The crystal models of m-TTP also showed a slipped $\pi - \pi$ stacking structure, while the t-TTP models showed approximately the same cell parameter and packing structure as anthracen [42, 43], although the shortest $S - S$ distances are found to be 3.69 Å and 4.06 Å for the m-TTP system. The $\pi - \pi$ intermolecular distances and the $S - S$ distances are slightly varied by introducing fluorine and bromine substituents. A comparison of the box dimensions of the different crystal models shows that the cell parameters are affected by introducing different numbers of heteroatom (F, Br) at different locations into the TTP precursors.

3.2. Electronic properties

3.2.1. Density of states

Figure 3 shows the calculated density of states (DOSs) for molecular (solid red curve) and crystal (dashed blue curve) structures of tetrathienophenazine derivatives and their fluorinated and brominated derivatives. The DOSs of the l-TTP, m-TTP and t-TTP molecules shows that the position and the shape of different occupied and unoccupied peaks are strongly affected by changing the position of the sulfur atoms. In the m-TTP model, the

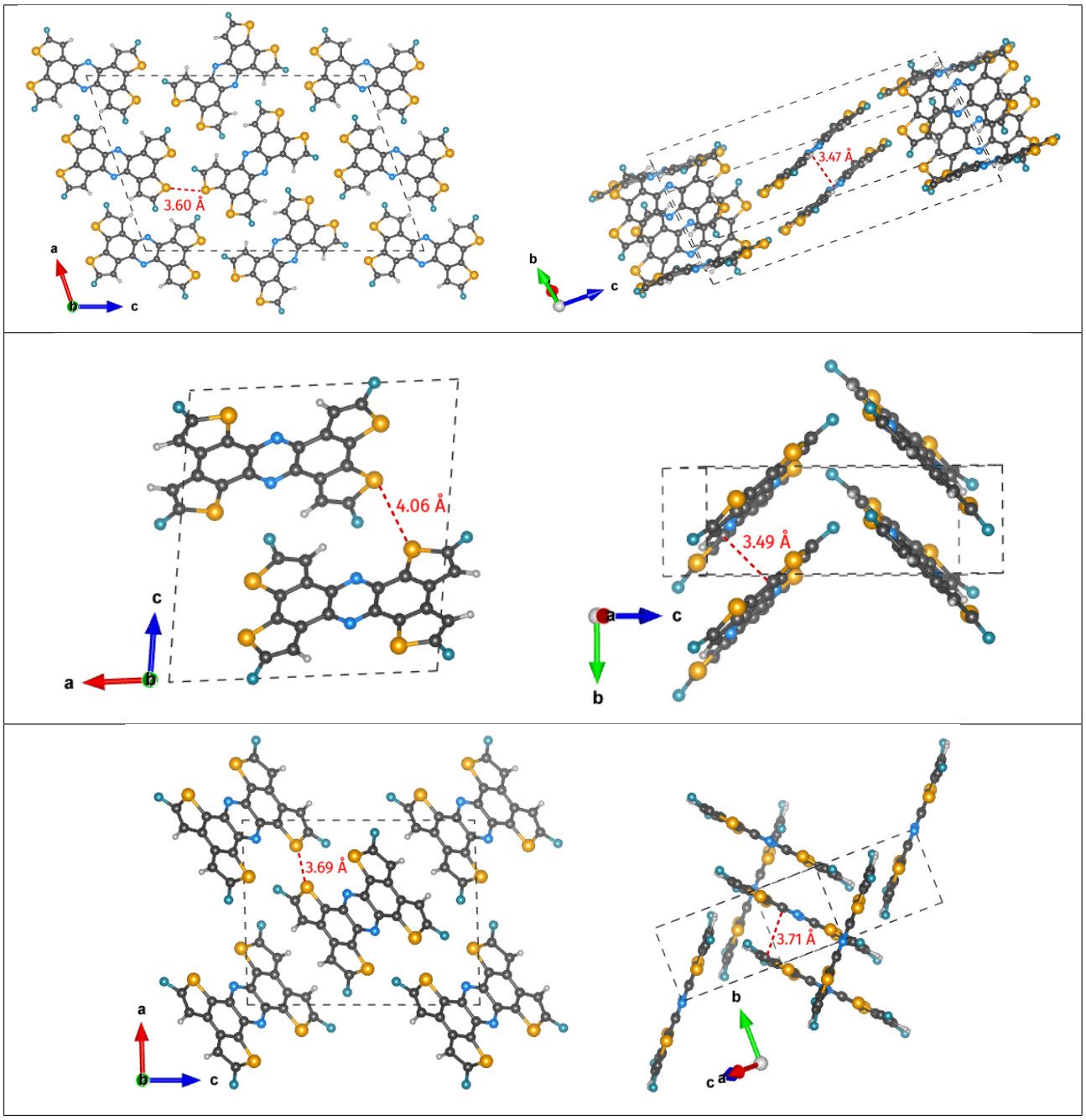

Figure 2: Top and side views of l-TTP (upper panel), m-TTP (middle panel) and t-TTP (lower panel) crystals. The primitive cell of l-TTP crystal contains 4 molecules, however, for m-TTP and t-TTP crystals, each one contains 2 molecules. The S-S (in left panels) and $\pi - \pi$ (in right panels) distances are shown in red.

peaks of the unoccupied states shift to the Fermi level as compared to those of l-TTP which must be due to the change of the position of the two sulfur atoms towards the inside. A slight positive upward displacement in the energies of the occupied states has been observed

Table 1: Crystal cell parameters of TTP derivatives and their fluorine and bromine substituents systems computed within GGA/PBE+vdW approximation.

	a (Å)	b (Å)	c (Å)	$\beta(^\circ)$
l-TTP	17.06	3.89	25.72	108.8
l-TTP1	17.12	4.08	25.86	109.0
l-TTP2	17.03	3.89	25.78	109.0
l-TTP3	17.09	3.90	25.78	109.0
l-TTP4	17.36	3.99	25.92	109.1
m-TTP	12.58	4.82	13.72	96.6
m-TTP1	12.78	4.82	13.63	97.0
m-TTP2	12.75	4.96	13.72	96.7
m-TTP3	12.59	4.85	13.72	96.7
m-TTP4	12.75	4.96	13.72	96.7
t-TTP	11.25	5.01	14.17	91.7
t-TTP1	11.48	5.08	14.26	91.7
t-TTP2	11.89	5.02	14.18	91.9
t-TTP3	11.75	5.09	14.19	91.9
t-TTP4	11.36	5.02	14.22	91.8

as well. This reduces the band gap from 2.65 eV to 2.32 eV. When the four sulfur atoms are located inside (t-TTP model), the shape of the occupied states is clearly modified, it becomes narrower with a slight displacement to the Fermi level compared to that of the m-TTP model. The band gap of this model grows to 2.54 eV due to the displacement of the peaks of unoccupied states to positive energies. The calculated m-TTP band gap is in agreement with those found by Xie et al. [30], while a slight difference is found for the l-TTP and t-TTP band gaps, probably because we are using a different functional.

For the crystal structure of the three derivatives, we observed a broadening of most occupied and unoccupied peaks and a shift to the Fermi level depending on the location of the sulfur atoms. As expected, the bandgaps in the cristalline structures are reduced compared to the HOMO-LUMO gaps of the isolated molecules. Specifically they are reduced to 1.46 eV, 1.60 and 1.56 eV for l-TTP, m-TTP and t-TTP, respectively (see Table 2). The reduction of the band gaps depends on the $S-S$ interactions. The band gap of the l-TTP derivative where the sulfur atoms are located outside is lower than in m-TTP and t-TTP, probably because it has more $S-S$ interactions. For the molecular models, attaching the fluorine substituents introduces a shift of the peaks of the unoccupied states to positive energies and a slight shift of the occupied ones to negative energies. This results in an increase in band gap for most derivatives. However, the substitution of hydrogen by bromine atoms modifies

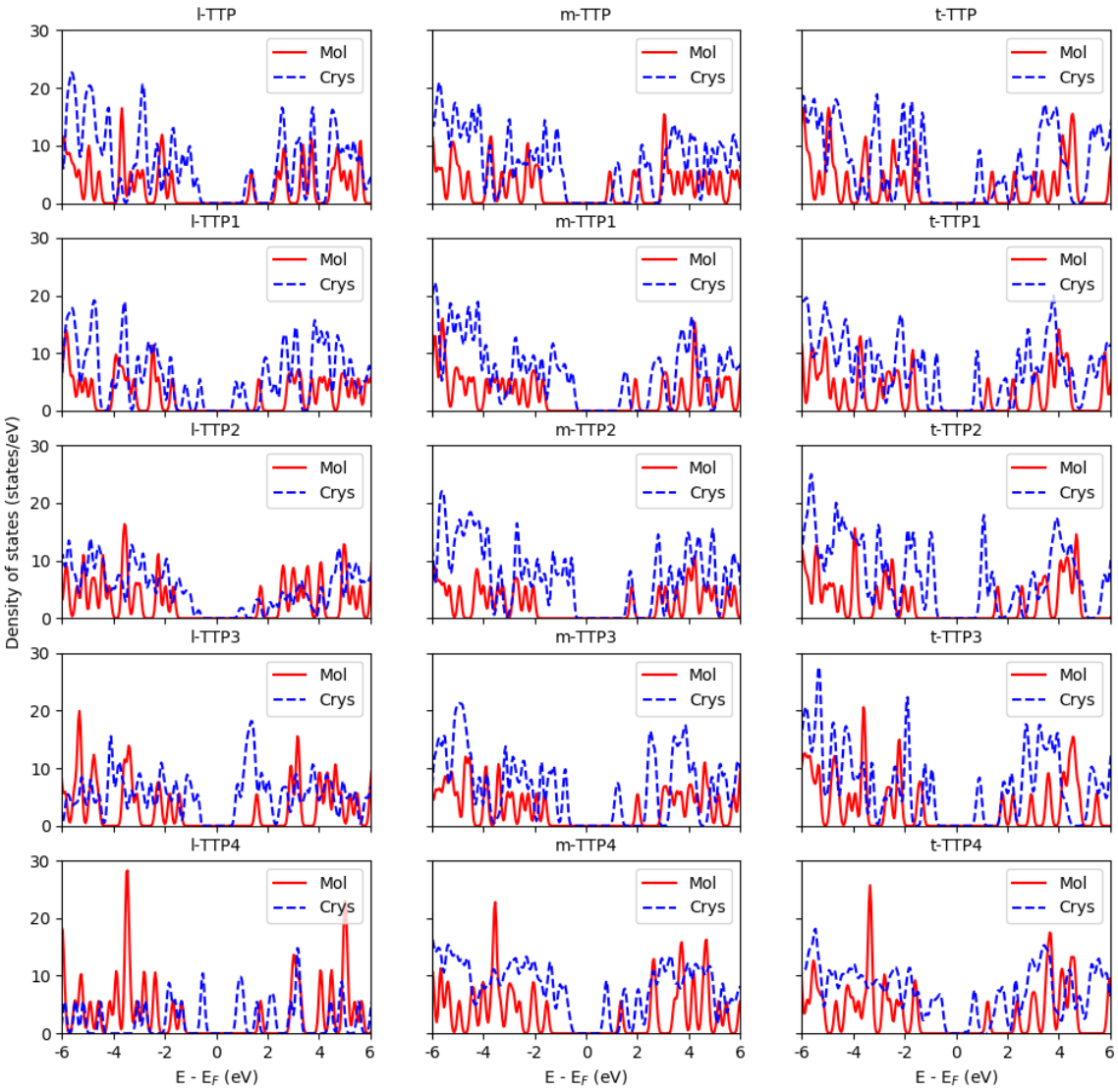

Figure 3: GGA/PBE+vdW calculated DOSs for molecular (solid red curve) and crystal structure (dashed blue curve) of tetrathienophenazine derivatives (l-TTP, m-TTP and t-TTP) and their fluorine and bromine substituents systems. The Fermi level (E_F) is the zero of energy.

the band gap only very slightly.

For crystals, both fluorination and bromination of the precursor TTP crystals reduce significantly the HOMO-LUMO band gaps of the three derivatives, which is in agreement with the results for ATT crystals computed by J. Yin and co-workers [22]. This reduction is probably due to the intermolecular interaction between different substituents (F–F or Br–Br). Table 2 shows that the m-TTP derivatives have higher band gaps compared to those found for l-TTP and t-TTP derivatives. In addition, we found that the fluorinated l-TTP derivatives give lower band gaps compared to those of m-TTP and t-TTP while the

Table 2: Computed band gaps (in eV) for molecules and crystals structure of tetrathienophenazine derivatives and their fluorine and bromine substituents using the GGA/PBE+vdW approximation.

Systems	**Gap(eV)**		Systems	**Gap(eV)**		Systems	**Gap(eV)**	
	Molecule	Crystal		Molecule	Crystal		Molecule	Crystal
l-TTP	2.65	1.46	m-TTP	2.32	1.60	t-TTP	2.54	1.56
l-TTP1	2.94	0.91	m-TTP1	3.35	1.48	t-TTP1	2.48	1.05
l-TTP2	2.97	1.21	m-TTP2	3.41	1.77	t-TTP2	2.89	1.39
l-TTP3	2.56	1.17	m-TTP3	3.15	1.48	t-TTP3	2.71	1.24
l-TTP4	2.62	0.88	m-TTP4	2.41	0.96	t-TTP4	2.35	0.66

brominated t-TTP derivative has lower band gap compared to those of l-TTP and m-TTP. In all cases, the bromination has stronger effects than fluorination and leads to lower band gaps. We found that attaching electron-withdrawing substituents such as Br and F atoms to the π-conjugated ring influences the electronic properties. We conclude that the introduction of fluorine and bromine atoms in TTP derivatives reduces the HOMO-LUMO gaps, which is beneficial for electron/hole injection and provides charge carrier stabilization.

3.2.2. Band structure

The band structures along the high symmetry directions of l-TTP, m-TTP and t-TTP crystals and their derivatives are shown in Figure 4. In general, the appearance of either dispersive or flat bands is a reflection of the anisotropy in the charge transport of the crystal. A wide band with strong dispersion indicates significant carrier mobility, while a flat band correlates with low mobility [22, 27]. By comparing the band structure of l-TTP, m-TTP and t-TTP crystals (see Figure 4), we clearly observed that the l-TTP model has the strongest dispersion for both valence and conduction bands. A strong valence band dispersion occurs along XD, ΓA and ΓB directions, which correspond to the b-c plane in real space, indicating that l-TTP model present two-dimensional (2D) hole transport. The m-TTP crystal shows also the possibility of 2D charge transfer for holes, but less than in l-TTP because its bandwith is clearly lower. For t-TTP, the flat valence and conduction bands in all directions suggest that their hole and electron mobilities are very low compared with those of l-TTP and m-TTP crystals. A strongly dispersing conduction band is also observed in the l-TTP model, which indicates significant electron mobility. We found that l-TTP and t-TTP are direct bandgap semiconductors, while m-TTP is an indirect bandgap one. The valence and conduction bands of l-TTP consist of four sub-bands which is due to the presence of four inequivalent molecules in their primitive unit cell, while for m-TTP and t-TTP, both valence and conduction bands consist of two sub-bands on account of the two irreducible molecules in their unit cell. Our results show that the l-TTP crystal can act as an ambipolar organic material. We found that the $S-S$ interaction, increased by changing

the position of the four sulfur atoms, plays an important role in controlling the transport channel.

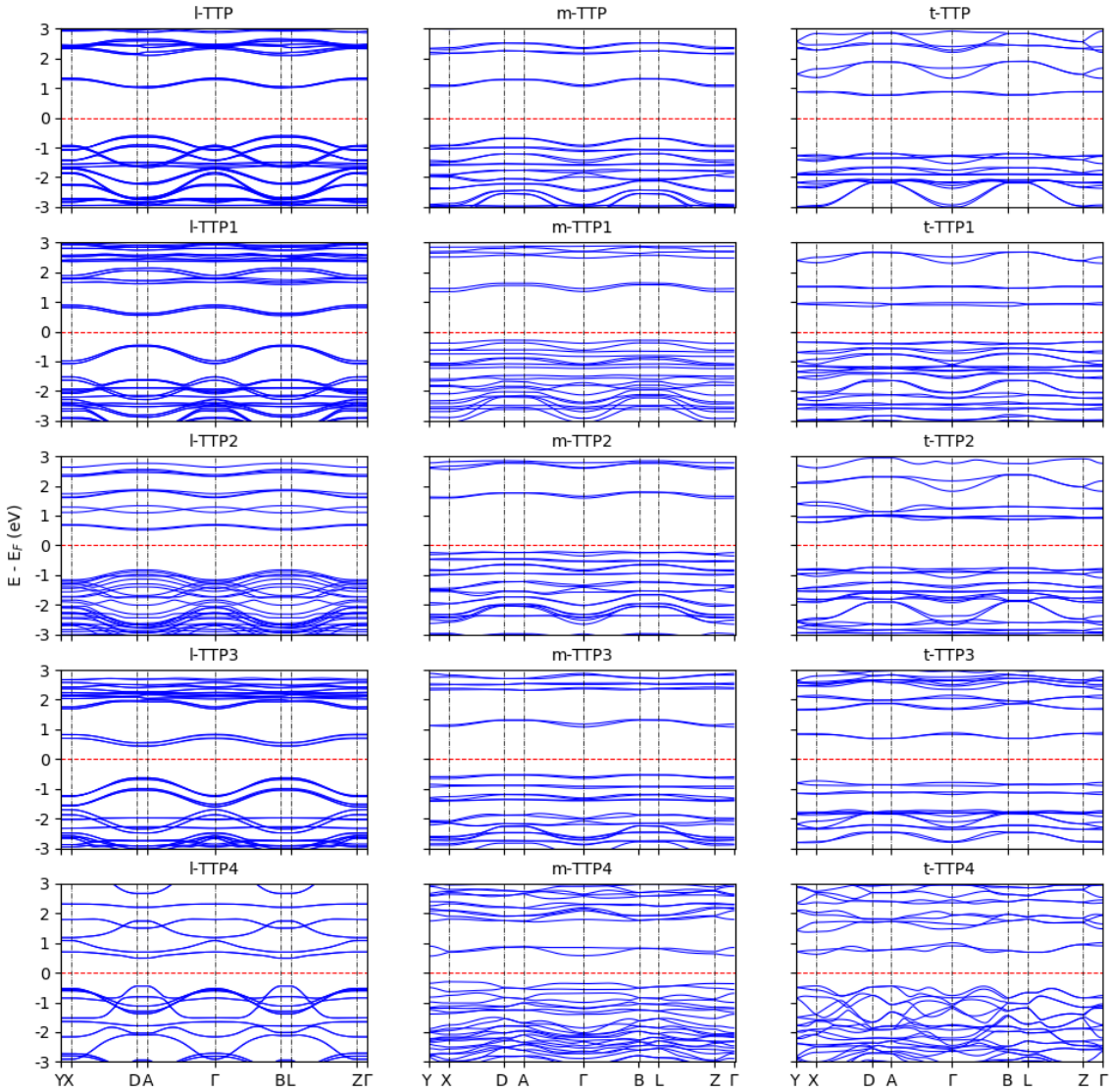

Figure 4: The band structure of the considered crystals computed within the GGA/PBE+vdW approximation. High symmetry k-points in the first Brillouin zone are $Y = (0.5; 0; 0)\frac{\pi}{a}$, $X = (0.5; 0; 0.5)\frac{\pi}{a}$, $D = (0.5; 0.5; 0.5)\frac{\pi}{a}$, $A = (0.5; 0.5; 0)\frac{\pi}{a}$, $\Gamma = (0; 0; 0)$, $B = (0; 0.5; 0)\frac{\pi}{a}$, $L = (0; 0.5; 0.5)\frac{\pi}{a}$, $Z = (0; 0; 0.5)\frac{\pi}{a}$. The Fermi level is set to zero.

The flat valence and conduction bands in all directions of the fluorinated m-TTP and t-TTP derivatives (see Figure 4) suggest that their hole and electron mobilities are very low. We found that the fluorination of the m-TTP and t-TTP precursor does not affect the hole and/or electron transport properties of these models. However, our calculations show also that the introduction of the fluorine atoms improves the hole mobility of the l-TTP precursor. The width of the valence band depends on the number and the location of the

fluorine substituents. Figure 4 shows that introducing the position of two fluorine atoms along the diagonal of the l-TTP molecule reduces the charge carrier mobility (l-TTP2). However, for the l-TTP1 and l-TTP3 models, the fluorine substituents increase the width of the valence band. The largest dispersion of the valence band occurs along the XD, ΓA and ΓB directions, and the valence band is broader than the conduction band. This suggests that holes are more mobile than electrons, and that l-TTP1 and l-TTP3 can act as hole transport materials. These crystals present also 2D electron transport, indicating that they can act as an ambipolar organic semiconductors. We therefore conclude that the number and the location of fluorine atoms introduced in the TTP derivative play an important role in controlling the transport channel. However, by introducing four bromine substituents in the l-TTP precursor, our calculation shows a strongly dispersing valence band in all directions and significant hole mobility. For m-TTP4 and t-TTP4 crystals, the wide valence and conduction bands in all direction suggest that their hole and electron mobilities are very high, and that the brominated derivatives are ambipolar organic materials. To conclude, our results indicate that l-TTP, l-TTP1, l-TTP3, l-TTP4, m-TTP4 and t-TTP4 are promising ambipolar organic materials, where the hole mobility is larger than the electron one.

3.3. Optical absorption properties

The optical properties of such system are generally studied by a complex dielectric function that depends on frequency $\varepsilon(\omega) = \varepsilon_1(\omega) + i\varepsilon_2(\omega)$, where $\varepsilon_1(\omega)$ and $\varepsilon_2(\omega)$ are its real and imaginary parts. $\varepsilon(\omega)$ describes the linear response of the system to electromagnetic radiation, which is related to the interaction of photons with electrons and optical transitions of the considered systems [44, 45]. The imaginary part of the dielectric function $\varepsilon_2(\omega)$ can be computed by the momentum matrix between the occupied and unoccupied wave functions [46, 47]. The real part $\varepsilon_1(\omega)$ can be determined from the imaginary part $\varepsilon_2(\omega)$ by applying the Kramers-Kronig relationship [41]. The variation of the real and imaginary parts of the dielectric function with energy is represented in Figure 5. The static real part of the dielectric function $\varepsilon_1(\omega)$ is given in Table 3 for all considered systems. From Table 3, by comparing the calculated values of $\varepsilon_1(0)$ of l-TTP, m-TTP and t-TTP isomers, we found that l-TTP has the maximum $\varepsilon_1(0)$, whereas t-TTP has the least value. We conclude that l-TTP isomer shows the best optical screening whereas the t-TTP derivative has the poorest one. Our results show that the optical properties are affected by changing the position of the sulfur atoms. Attaching fluorine substituents to the m-TTP and t-TTP isomers has small effects on the static dielectric constant, while attaching the bromine substituents increases $\varepsilon_1(0)$. M-TTP4 and t-TTP4 show good optical response. For the l-TTP derivatives, our results show that l-TTP, l-TTP1, l-TTP3 and l-TTP4 have the best optical response. In Figure 5, each $\varepsilon_1(\omega)$ spectrum shows two main peaks at about 1.6 and 2.5 eV for l-TTP, 1.7 and 2.3 eV for m-TTP and 1.6 and 2.4 eV for t-TTP. The oscillatory behavior of each of the TTP derivative is very clear for the real part up to 3 eV. Beyond 3 eV, the optical response becomes very poor and all curves merge. Two main peaks are also observed in the $\varepsilon_2(\omega)$ around 1.6 and 2.4 eV for l-TTP, 1.7 and 2.3 eV for m-TTP and 1.8 and 2.7 eV for t-TTP. The two peaks originate from the optical transition between the occupied and unoccupied bands. For the best optical response, by attaching electron-withdrawing substituents (F,

Figure 5: Computed GGA/PBE+vdW imaginary (solid red curve) and real parts (dashed blue curve) of dielectric function (ε) according to energy in eV of l-TTP derivatives (left panel), m-TTP derivatives (middle panel) and t-TTP derivatives (right panel).

Br), our results show that the two peaks of both $\varepsilon_1(\omega)$ and $\varepsilon_2(\omega)$ are displaced to lower energies compared to the TTP precursors, while for the poor optical response, these peaks are displaced to higher energies. L-TTP, l-TTP1, l-TTP3, l-TTP4, m-TTP4 and t-TTP4 crystals have the best optical response which is consistent with their electronic properties.

4. Conclusions

In this work, we predicted the optoelectronic properties of crystals of TTP derivatives and their alkyl-substituted derivatives by means of density functional theory within the

Table 3: The calculated static dielectric constant $\varepsilon(0)$ of tetrathienophenazine derivatives and their alkyl-substituted derivatives using the GGA/PBE+vdW approximation.

$\varepsilon(0)$	l-TTP	m-TTP	t-TTP
TTP	5.80	3.72	2.92
TTP1	4.03	3.63	2.89
TTP2	3.73	3.63	2.90
TTP3	6.03	3.69	2.80
TTP4	5.14	4.58	3.47

GGA/PBE+vdW approximation. Our study shows that the optical, electronic and transport properties of TTP derivatives are affected by changing the location of the sulfur atoms. We found that the l-TTP crystal is a promising ambipolar organic semiconductor. We have confirmed that attaching electron-withdrawing substituents such as fluorine and bromine changes their optical and electrochemical properties. We have shown that the introduction of fluorine and bromine atoms in TTP derivatives lowers the HOMO-LUMO gaps, which is beneficial to electron and/or hole injection and provides charge carrier stabilization. We found that the introduction of fluorine atoms improves hole transport only in l-TTP derivative. However, the incorporation of the bromine atoms improves both hole and electron transport. We conclude from our band structure results that l-TTP, l-TTP1, l-TTP3, l-TTP4, m-TTP4 and t-TTP4 are promising ambipolar organic materials, where the hole transfer ability is superior to the electron one. The computed dielectric function confirms that l-TTP, l-TTP1, l-TTP3, l-TTP4, m-TTP4 and t-TTP4 crystals have the best optical response. We found that bromination has a larger effect than fluorination on their optical and electronic properties.

Acknowledgments

We would like to acknowledge fruitful discussion with Sébastien Lebègue and his group.

References

[1] J. Huang, J.-H. Su, H. Tian, The development of anthracene derivatives for organic light-emitting diodes, J. Mater. Chem. 22 (2012) 10977–10989. doi:10.1039/C2JM16855C.
URL http://dx.doi.org/10.1039/C2JM16855C

[2] G. Gigli, G. Barbarella, L. Favaretto, F. Cacialli, R. Cingolani, High-efficiency oligothiopene-based light-emitting diodes, Applied Physics Letters 75 (4) (1999) 439–441. arXiv:https://doi.org/10.1063/1.124403, doi:10.1063/1.124403.
URL https://doi.org/10.1063/1.124403

[3] A. Heckmann, C. Lambert, Angewandte Chemie International Edition 51 (2012) 326–392. doi:10.1002/anie.201100944, [link].
URL http://dx.doi.org/10.1002/anie.201100944

[4] S.-C. Lo, P. L. Burn, Chemical Reviews 107 (2007) 1097–1116. arXiv:http://dx.doi.org/10.1021/cr050136l, doi:10.1021/cr050136l, [link].
URL http://dx.doi.org/10.1021/cr050136l

[5] Y. Qiao, Y. Guo, C. Yu, F. Zhang, W. Xu, Y. Liu, D. Zhu, Diketopyrrolopyrrole-containing quinoidal small molecules for high-performance, air-stable, and solution-processable n-channel organic field-effect transistors, Journal of the American Chemical Society 134 (9) (2012) 4084–4087, pMID: 22352880. arXiv:https://doi.org/10.1021/ja3003183, doi:10.1021/ja3003183.
URL https://doi.org/10.1021/ja3003183

[6] H. Moon, R. Zeis, E.-J. Borkent, C. Besnard, A. J. Lovinger, T. Siegrist, C. Kloc, Z. Bao, Synthesis, crystal structure, and transistor performance of tetracene derivatives, Journal of the American Chemical Society 126 (47) (2004) 15322–15323, pMID: 15563126. arXiv:https://doi.org/10.1021/ja045208p, doi:10.1021/ja045208p.
URL https://doi.org/10.1021/ja045208p

[7] R. P. Ortiz, J. Casado, V. Hernández, J. L. Navarrete, J. Letizia, M. Ratner, A. Facchetti, T. Marks, Thiophene-diazine molecular semiconductors: Synthesis, structural, electrochemical, optical, and electronic structural properties; implementation in organic field-effect transistors, Chemistry - A European Journal 15 (20) 5023–5039. arXiv:https://onlinelibrary.wiley.com/doi/pdf/10.1002/chem.200802424, doi:10.1002/chem.200802424.
URL https://onlinelibrary.wiley.com/doi/abs/10.1002/chem.200802424

[8] Y. Geng, H.-B. Li, S.-X. Wu, Z.-M. Su, The interplay of intermolecular interactions, packing motifs and electron transport properties in perylene diimide related materials: a theoretical perspective, J. Mater. Chem. 22 (2012) 20840–20851. doi:10.1039/C2JM33369D.
URL http://dx.doi.org/10.1039/C2JM33369D

[9] A. Saeki, Y. Koizumi, T. Aida, S. Seki, Accounts of Chemical Research 45 (2012) 1193–1202. arXiv:http://dx.doi.org/10.1021/ar200283b, doi:10.1021/ar200283b, [link].
URL http://dx.doi.org/10.1021/ar200283b

[10] M. L. Tang, Z. Bao, Chemistry of Materials 23 (2011) 446–455. arXiv:http://dx.doi.org/10.1021/cm102182x, doi:10.1021/cm102182x, [link].
URL http://dx.doi.org/10.1021/cm102182x

[11] Y. Lin, Y. Li, X. Zhan, Small molecule semiconductors for high-efficiency organic photovoltaics, Chem. Soc. Rev. 41 (2012) 4245–4272. doi:10.1039/C2CS15313K.
URL http://dx.doi.org/10.1039/C2CS15313K

[12] Z. B. Henson, K. Müllen, G. C. Bazan, Design strategies for organic semiconductors beyond the molecular formula, Nature chemistry 4 (9) (2012) 699.

[13] Y.-A. Duan, Y. Geng, H.-B. Li, J.-L. Jin, Y. Wu, Z.-M. Su, Theoretical characterization and design of small molecule donor material containing naphthodithiophene central unit for efficient organic solar cells, Journal of Computational Chemistry 34 (19) 1611–1619. arXiv:https://onlinelibrary.wiley.com/doi/pdf/10.1002/jcc.23298, doi:10.1002/jcc.23298.
URL https://onlinelibrary.wiley.com/doi/abs/10.1002/jcc.23298

[14] C. Li, H. Wonneberger, Advanced Materials 24 (2012) 613–636. doi:10.1002/adma.201104447, [link].
URL http://dx.doi.org/10.1002/adma.201104447

[15] X. Zhan, D. Zhu, Polym. Chem. 1 (2010) 409–419. doi:10.1039/B9PY00325H, [link].
URL http://dx.doi.org/10.1039/B9PY00325H

[16] T. W. Holcombe, C. H. Woo, D. F. Kavulak, B. C. Thompson, J. M. J. Fréchet, Journal of the American Chemical Society 131 (2009) 14160–14161. arXiv:http://dx.doi.org/10.1021/ja9059359, doi:10.1021/ja9059359, [link].
URL http://dx.doi.org/10.1021/ja9059359

[17] S. R. Forrest, The path to ubiquitous and low-cost organic electronic appliances on plastic, Nature 428 (6986) (2004) 911.

[18] M. Mas-Torrent, C. Rovira, Role of molecular order and solid-state structure in organic field-effect transistors, Chemical Reviews 111 (8) (2011) 4833–4856, pMID: 21417271. arXiv:https://doi.org/10.1021/cr100142w, doi:10.1021/cr100142w.
URL https://doi.org/10.1021/cr100142w

[19] P. Cudazzo, F. Sottile, A. Rubio, M. Gatti, Journal of Physics: Condensed Matter 27 (2015) 113204.

[link].
URL http://stacks.iop.org/0953-8984/27/i=11/a=113204
[20] K. Hummer, C. Ambrosch-Draxl, Phys. Rev. B 72 (2005) 205205. doi:10.1103/PhysRevB.72.205205, [link].
URL https://link.aps.org/doi/10.1103/PhysRevB.72.205205
[21] P. F. Baude, D. A. Ender, M. A. Haase, T. W. Kelley, D. V. Muyres, S. D. Theiss, Pentacene-based radio-frequency identification circuitry, Applied Physics Letters 82 (22) (2003) 3964–3966. arXiv:https://doi.org/10.1063/1.1579554, doi:10.1063/1.1579554.
URL https://doi.org/10.1063/1.1579554
[22] J. Yin, K. Chaitanya, X.-H. Ju, Theoretical investigation of fluorination effect on the charge carrier transport properties of fused anthra-tetrathiophene and its derivatives, Journal of Molecular Graphics and Modelling 64 (2016) 40–50.
[23] J. C. Sancho-García, A. J. Pérez-Jiménez, Y. Olivier, J. Cornil, Molecular packing and charge transport parameters in crystalline organic semiconductors from first-principles calculations, Phys. Chem. Chem. Phys. 12 (2010) 9381–9388. doi:10.1039/B925652K.
URL http://dx.doi.org/10.1039/B925652K
[24] S. Chai, S.-H. Wen, J.-D. Huang, K.-L. Han, Density functional theory study on electron and hole transport properties of organic pentacene derivatives with electron-withdrawing substituent, Journal of Computational Chemistry 32 (15) 3218–3225. arXiv:https://onlinelibrary.wiley.com/doi/pdf/10.1002/jcc.21904, doi:10.1002/jcc.21904.
URL https://onlinelibrary.wiley.com/doi/abs/10.1002/jcc.21904
[25] W. Wu, Y. Liu, D. Zhu, π-conjugated molecules with fused rings for organic field-effect transistors: design, synthesis and applications, Chem. Soc. Rev. 39 (2010) 1489–1502. doi:10.1039/B813123F.
URL http://dx.doi.org/10.1039/B813123F
[26] C. Röger, F. Würthner, Core-tetrasubstituted naphthalene diimides: synthesis, optical properties, and redox characteristics, The Journal of Organic Chemistry 72 (21) (2007) 8070–8075, pMID: 17887710. arXiv:https://doi.org/10.1021/jo7015357, doi:10.1021/jo7015357.
URL https://doi.org/10.1021/jo7015357
[27] Y.-A. Duan, H.-B. Li, Y. Geng, Y. Wu, G.-Y. Wang, Z.-M. Su, Theoretical studies on the hole transport property of tetrathienoarene derivatives: The influence of the position of sulfur atom, substituent and π-conjugated core, Organic Electronics 15 (2) (2014) 602–613.
[28] J. Yin, K. Chaitanya, X.-H. Ju, Bromination and cyanation for improving electron transport performance of anthra-tetrathiophene, Journal of Materials Research 31 (3) (2016) 337–347. doi:10.1557/jmr.2016.8.
[29] G. Giovannetti, G. Brocks, J. van den Brink, Phys. Rev. B 77 (2008) 035133. doi:10.1103/PhysRevB.77.035133, [link].
URL https://link.aps.org/doi/10.1103/PhysRevB.77.035133
[30] Y. Xie, T. Fujimoto, S. Dalgleish, Y. Shuku, M. M. Matsushita, K. Awaga, Synthesis, optical properties and charge transport characteristics of a series of novel thiophene-fused phenazine derivatives, Journal of Materials Chemistry C 1 (21) (2013) 3467–3481.
[31] I. A. Fedorov, Materials Chemistry and Physics 199 (Supplement C) (2017) 173 – 178. doi:https://doi.org/10.1016/j.matchemphys.2017.06.060, [link].
URL http://www.sciencedirect.com/science/article/pii/S0254058417305023
[32] I. A. Fedorov, Y. N. Zhuravlev, V. P. Berveno, Phys. Chem. Chem. Phys. 13 (2011) 5679–5686. doi:10.1039/C0CP02200D, [link].
URL http://dx.doi.org/10.1039/C0CP02200D
[33] J. M. Soler, E. Artacho, J. D. Gale, A. García, J. Junquera, P. Ordejón, D. Sánchez-Portal, Journal of Physics: Condensed Matter 14 (2002) 2745. [link].
URL http://stacks.iop.org/0953-8984/14/i=11/a=302
[34] D. Sánchez-Portal, P. Ordejon, E. Artacho, J. M. Soler, Density-functional method for very large systems with lcao basis sets, International journal of quantum chemistry 65 (5) (1997) 453–461.

[35] W. Kohn, L. Sham, doi: 10.1103/physrev. 140. a1133, Phys. Rev. A 140 (1965) 113.
[36] J. P. Perdew, K. Burke, M. Ernzerhof, Phys. Rev. Lett. 77 (1996) 3865–3868.
[37] N. Troullier, J. L. Martins, Phys. Rev. B 43 (1991) 1993–2006. doi:10.1103/PhysRevB.43.1993, [link].
URL https://link.aps.org/doi/10.1103/PhysRevB.43.1993
[38] L. Kleinman, D. Bylander, Efficacious form for model pseudopotentials, Physical Review Letters 48 (20) (1982) 1425.
[39] S. Grimme, Semiempirical gga-type density functional constructed with a long-range dispersion correction, Journal of Computational Chemistry 27 (15) 1787–1799. arXiv:https://onlinelibrary.wiley.com/doi/pdf/10.1002/jcc.20495, doi:10.1002/jcc.20495.
URL https://onlinelibrary.wiley.com/doi/abs/10.1002/jcc.20495
[40] J. D. Pack, H. J. Monkhorst, Phys. Rev. B 16 (1977) 1748–1749. doi:10.1103/PhysRevB.16.1748, [link].
URL https://link.aps.org/doi/10.1103/PhysRevB.16.1748
[41] R. de L. Kronig, J. Opt. Soc. Am. 12 (1926) 547–557. doi:10.1364/JOSA.12.000547, [link].
URL http://www.osapublishing.org/abstract.cfm?URI=josa-12-6-547
[42] J. L. Brusso, O. D. Hirst, A. Dadvand, S. Ganesan, F. Cicoira, C. M. Robertson, R. T. Oakley, F. Rosei, D. F. Perepichka, Chemistry of Materials 20 (2008) 2484–2494. arXiv:http://dx.doi.org/10.1021/cm7030653, doi:10.1021/cm7030653, [link].
URL http://dx.doi.org/10.1021/cm7030653
[43] W.-J. Liu, Y. Zhou, Y. Ma, Y. Cao, J. Wang, J. Pei, Thin film organic transistors from air-stable heteroarenes: anthra[1,2-b:4,3-b:5,6-b:8,7-b]tetrathiophene derivatives, Organic Letters 9 (21) (2007) 4187–4190, pMID: 17850155. arXiv:https://doi.org/10.1021/ol701690y, doi:10.1021/ol701690y.
URL https://doi.org/10.1021/ol701690y
[44] R. King-Smith, D. Vanderbilt, Theory of polarization of crystalline solids, Physical Review B 47 (3) (1993) 1651.
[45] S. Sharma, C. Ambrosch-Draxl, Second-harmonic optical response from first principles, Physica Scripta T109 (2004) 128. doi:10.1238/physica.topical.109a00128.
URL https://doi.org/10.1238%2Fphysica.topical.109a00128
[46] D.-D. Sang, Q.-L. Wang, C. Han, K. Chen, Y.-W. Pan, Electronic and optical properties of lithium niobate under high pressure: A first-principles study, Chinese Physics B 24 (7) (2015) 077104. doi:10.1088/1674-1056/24/7/077104.
URL https://doi.org/10.1088%2F1674-1056%2F24%2F7%2F077104
[47] C. N. M. Ouma, S. Singh, K. O. Obodo, G. O. Amolo, A. H. Romero, Controlling the magnetic and optical responses of a mos2 monolayer by lanthanide substitutional doping: a first-principles study, Phys. Chem. Chem. Phys. 19 (2017) 25555–25563. doi:10.1039/C7CP03160B.
URL http://dx.doi.org/10.1039/C7CP03160B